Supplementary material for

Stimulation of the cuneiform nucleus enables training and boosts recovery after spinal cord injury

Anna-Sophie Hofer,[1,2,3] Myriam I. Scheuber,[1,2,3] Andrea M. Sartori,[1,2,3,†] Nicolas Good,[1,2,3] Stephanie A. Stalder,[1,3] Nicole Hammer,[2,3] Kai Fricke,[1,3] Sina M. Schalbetter,[1,2,3] Anne K. Engmann,[1,3,#] Rebecca Z. Weber,[1,2,3] Ruslan Rust,[1,2,3] Marc P. Schneider,[1,3] Natalie Russi,[1,3] Giacomin Favre[4] and Martin E. Schwab[1,2,3]

Author affiliations:

1 Brain Research Institute, University of Zurich, 8057 Zurich, Switzerland

2 Institute for Regenerative Medicine, University of Zurich, 8952 Schlieren, Switzerland

3 Department of Health Sciences and Technology, ETH Zurich, 8092 Zurich, Switzerland

4 Department of Economics, University of Zurich, 8032 Zurich, Switzerland

† Current address: Department of Medicine, Harvard Medical School, Beth Israel Deaconess Medical Center, Boston, USA

Current address: Department of Stem Cell and Regenerative Biology at Harvard University, Cambridge, USA

Correspondence to: Anna-Sophie Hofer

Institute for Regenerative Medicine, University of Zurich, Wagistrasse 12, 8952 Schlieren, Switzerland

E-mail: hofer@irem.uzh.ch

Supplementary methods

DBS electrodes

Monopolar, 000-gauge stainless steel DBS electrodes isolated with parylene were implanted into the left CNF stereotaxically. Electrode shaft and two fine grounding silver-wires were connected to a 3-pin plug. Impedance of all electrodes was measured with an LCR-/ESR-meter (PeakTech® 2170), and only electrodes with an impedance of < 35 kΩ were used. Mean impedance of implanted electrodes was 13.77 ± 6.21 kΩ.

Definition of kinematic parameters

Speed is the horizontal movement velocity. Stepping frequency is the number of step cycles per second. Stepping speed is the horizontal hindlimb velocity. Protractive paw speed indicates the average horizontal MTP speed relative to the ipsilateral hip joint during swing phase. Step cycle duration reflects the time interval between two subsequent unilateral limb onsets. Stance phase duration indicates the time interval between ipsilateral stance onset and swing onset. Swing phase duration indicates the duration between ipsilateral swing onset and stance onset. Temporal step asynchrony reflects the temporal distance of right paw onset to closest left paw onset divided by right step cycle duration. Temporal step synchronization gives the deviation from the theoretical, perfect asynchrony value of 0.5 in percent in intact animals (called hindlimb synchronization). Hip height is the perpendicular distance of the hip joint from the runway at the mid-stance phase. Step width (base of support) is the sum of perpendicular distances of left and right heel at limb onset to body midline. During swimming, we measured the distance between right eye and water surface during stroke onset (called diving).

Supplementary figures

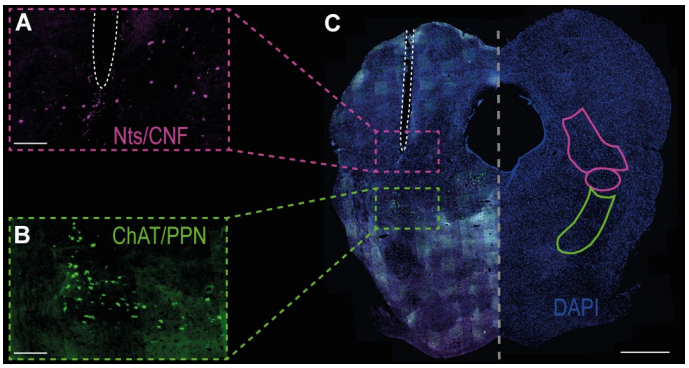

Supplementary Figure 1. Electrode positioning in the cuneiform nucleus of the left mesencephalic locomotor region. Anatomically correct electrode positioning was verified in randomly selected animals by in-situ hybridization for neurotensin (Nts) and choline acetyltransferase (ChAT) according to the protocols from RNAScope (Advanced Cell Diagnosis). Sequences of target, preamplifier, amplifier, and probes are proprietary and commercially available. Neurotensin[1,2] labels the cuneiform nucleus (CNF), ChAT[3] labels the pedunculopontine nucleus (PPN). (**A-C**) Representative images of fluorescent in-situ hybridization for mRNA of neurotensin (Cy3, magenta) and ChAT (Cy5, green) counterstained with DAPI (blue) illustrating electrode tip placement within the CNF and preservation of tissue structure after repeated CNF-DBS. (**A**) Magnification of neurotensin labeled cells of the left CNF surrounding the electrode tip (area surrounded by white dashed line). Scale bar: 200 µm. (**B**) Magnification of ChAT-positive cells of the left PPN. Scale bar: 200 µm. (**C**) Left: Illustration of electrode (highlighted by white dashed line) tip placement within the left cuneiform nucleus on triple-stained (Nts, ChAT, DAPI) coronal midbrain section of one representative animal at AP -7.8 mm. Right: DAPI only. Area highlighted in magenta represents CNF, green area represents PPN (landmarks based on Paxinos et al.[4]). Scale bar: 1 mm. Gray dashed vertical line represents midline.

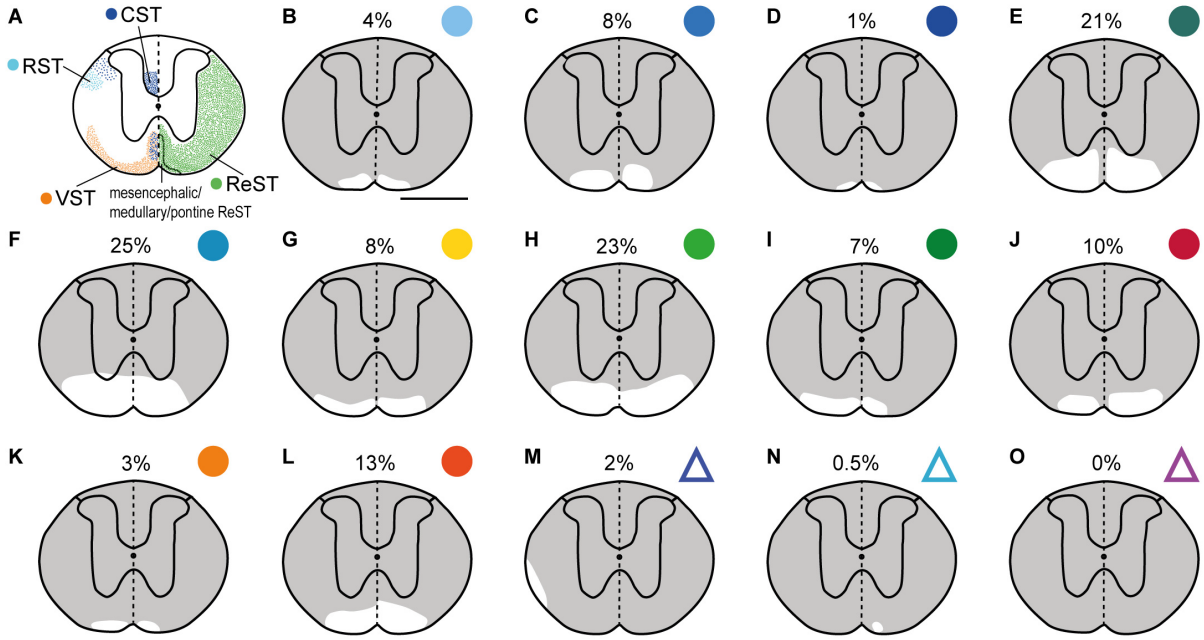

Supplementary Figure 2. Reconstructions of individual animals' lesion sites at thoracic level T10. (A) Schematic illustration of the distribution of the main descending tracts in the intact spinal cord at spinal level T10 based on a spinal cord atlas[5] and neuroanatomical studies.[6] CST (blue) = corticospinal tract. RST (light blue) = rubrospinal tract. VST (orange) = vestibulospinal tract. ReST (green) = reticulospinal tracts, including mesencephalic, medullary, and pontine fibers. (**B-O**) Individual reconstructions of spared (white) and destroyed (gray) tissue at the site of maximum lesion extent. Fraction of spared tissue of spinal cord cross section is shown in %. Scale bar: 1 mm. (**B-L**) Reconstructed, individual lesion sizes of animals represented by dots in Fig. 2: 1% to 25% bilateral, ventromedial fiber sparing (n = 11). Color code of dots is consistent to Fig. 2. (**M-O**) Lesion size reconstruction of animals represented by triangle in Fig. 2: 0.5% to 2% unilateral fiber sparing (n = 2), or complete lesion (0%, n = 1). Color code of triangles is consistent to Fig. 2.

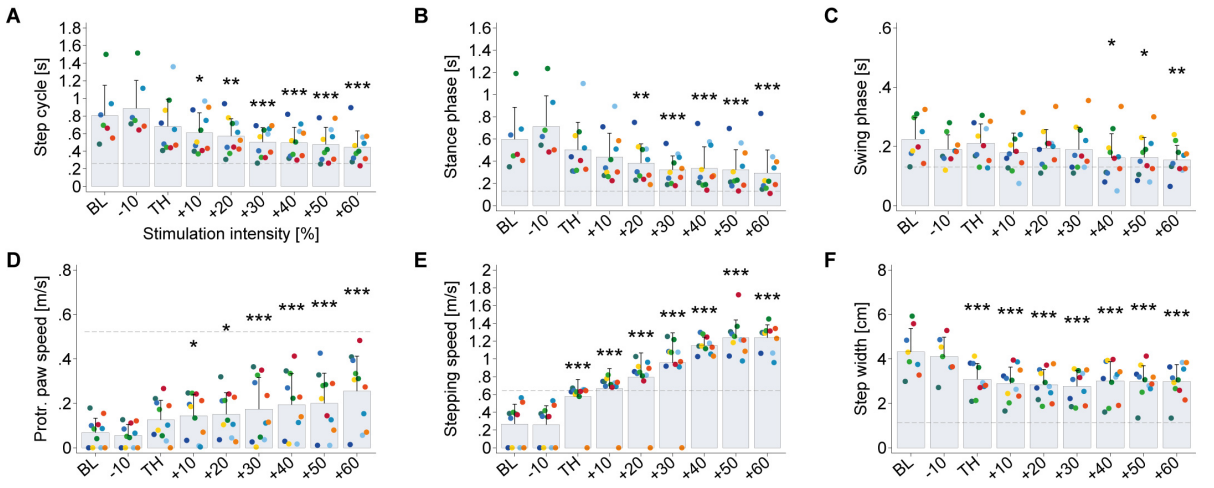

Supplementary Figure 3. Temporal execution of stepping improves with CNF-DBS 5 weeks after injury in an intensity-dependent manner. (**A-C**) CNF-DBS induces significant decrease in (**A**) step cycle duration (at ≥ TH+10%), (**B**) stance phase duration (at ≥ TH+20%), and (**C**) swing phase duration (at ≥ TH+40%), approaching intact animals' mean baseline levels (gray dashed horizontal lines). (**D** and **E**) Significant increase in (**D**) protractive (protr.) paw speed (at ≥ TH+10%), and (**E**) stepping speed (at ≥ TH) with CNF-DBS. (**F**) Animals were able to walk with a more physiological step width with CNF-DBS (≥ TH). Asterisks indicate significance of Bonferroni post hoc test comparing all parameters at each stimulation intensity with their baseline (0% stimulation) performance on dpi35 after one-way repeated measures (intensity) ANOVA ($P < 0.001$). * ($P < 0.05$), ** ($P < 0.01$), *** ($P < 0.001$). $n = 11$; animals with unilateral or no fiber sparing ($n = 3$) did not exhibit hindlimb step cycles upon CNF-DBS and thus had to be excluded from analysis of parameters shown in this figure. (**A-C** and **F**) Number of observations < 11 from BL to TH intensity as some animals only exhibited step cycles (required for determination of parameters) with suprathreshold stimulation. Data are represented as mean + SD, colored dots represent single animals. BL = baseline at day post injury 35 without DBS. TH = individual motor threshold. X-axis = stimulation intensity expressed as percent of TH.

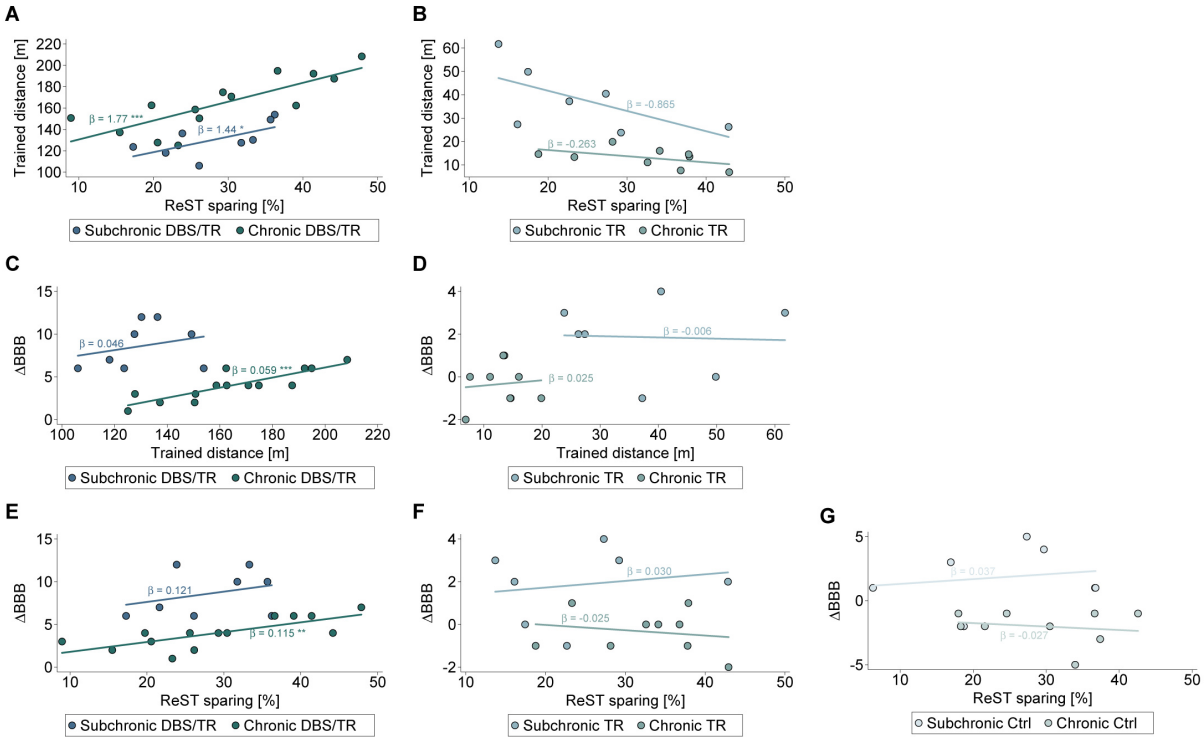

Supplementary Figure 4. Correlations of reticulospinal tract sparing, wading distance covered during training, and locomotor recovery in subchronic and chronic phase after SCI. (**A**) Significantly positive correlation of percent of spared reticulospinal tract (ReST) and trained distance in subchronic ($P < 0.05$; $n = 8$) and chronic ($P < 0.001$; $n = 14$) DBS/TR group. (**B**) No evidence for positive correlation between trained distance and ReST sparing in subchronic ($n = 7$) and chronic ($n = 9$) TR group ($P > 0.05$). (**C**) Linear regression of change in BBB score during training period on trained distance revealed a significantly positive correlation in chronic ($P < 0.001$; $n = 14$), and an insignificantly positive correlation in subchronic ($P > 0.05$; $n = 8$) DBS/TR group. (**D**) Insignificant correlation between change in BBB during training and trained distance in subchronic ($n = 7$) and chronic ($n = 9$) TR group ($P > 0.05$). (**E**) Regression of change in BBB score on percent of spared reticulospinal tract exhibits significantly larger gait improvements with smaller lesion sizes in the chronic ($P < 0.01$; $n = 14$) DBS/TR cohort and an insignificantly positive correlation in the subchronic ($P > 0.05$; $n = 8$) DBS/TR cohort. (**F**) No significant correlation between change in BBB and ReST sparing in subchronic ($n = 7$) and chronic ($n = 9$) TR group ($P > 0.05$). (**G**) No significant correlation of motor recovery and sparing of the ReST among subchronic ($n = 7$) and chronic ($n = 9$) Ctrl group ($P > 0.05$). Linear regressions were performed within each group in each cohort with robust standard errors. β = regression coefficient. * ($P < 0.05$), ** ($P < 0.01$), *** ($P < 0.001$).

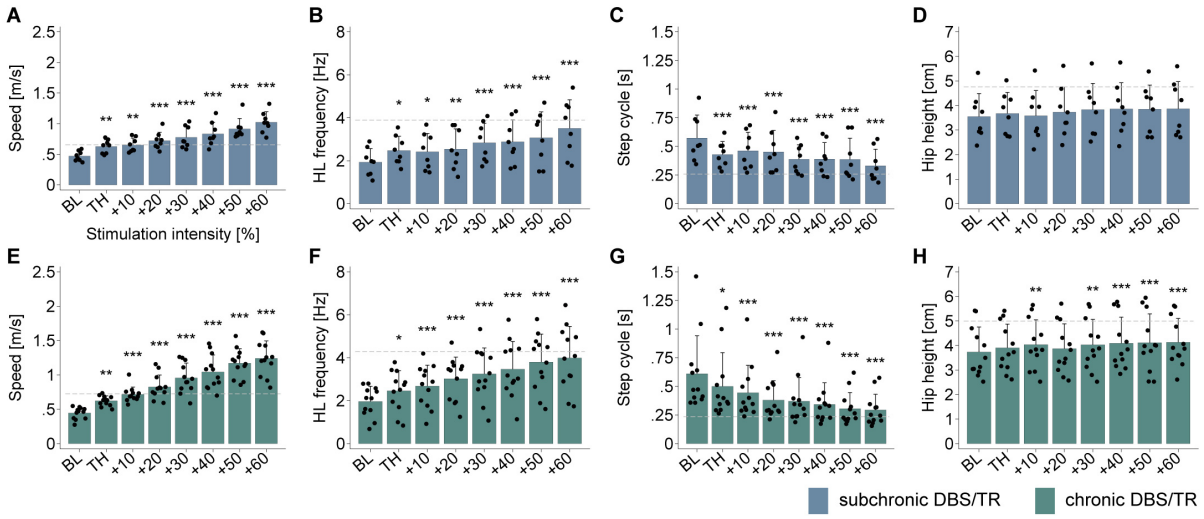

Supplementary Figure 5. Hindlimb locomotor function acutely improves with CNF-DBS even in very chronic stages of SCI. (**A-D**) Walking assessment without and with DBS in subchronic (blue) DBS/TR group at the end of retention period (dpi91; $n = 8$). Mean threshold intensity: 28.13 ± 8.67 µA. (**E-H**) Assessment of over-ground locomotion without and with DBS in chronic (green) DBS/TR group at the end of retention period (dpi154; $n = 12/14$, 2 animals excluded due to implant failure). Mean threshold intensity: 29.83 ± 8.78 µA. (**A** and **E**) Horizontal speed significantly increased with CNF-DBS at all stimulation intensities at both timepoints. (**B** and **F**) Significant increase in stepping frequency with stimulation intensity. (**C** and **G**) Step cycle duration significantly decreased with CNF-DBS. (**D** and **H**) Hip height was acutely affected by stimulation of the CNF in the chronic cohort on dpi154. Asterisks indicate significance of Bonferroni post hoc test comparing each parameter at each stimulation intensity with baseline performance after one-way repeated measures (intensity) ANOVA ($P < 0.001$). * ($P < 0.05$), ** ($P < 0.01$), *** ($P < 0.001$). BL = baseline without stimulation. TH = individual motor threshold. Data are represented as mean + SD. Dots represent single animals. Gray dashed line represents mean baseline value of intact animals. X-axis = stimulation intensity expressed as percent of TH.

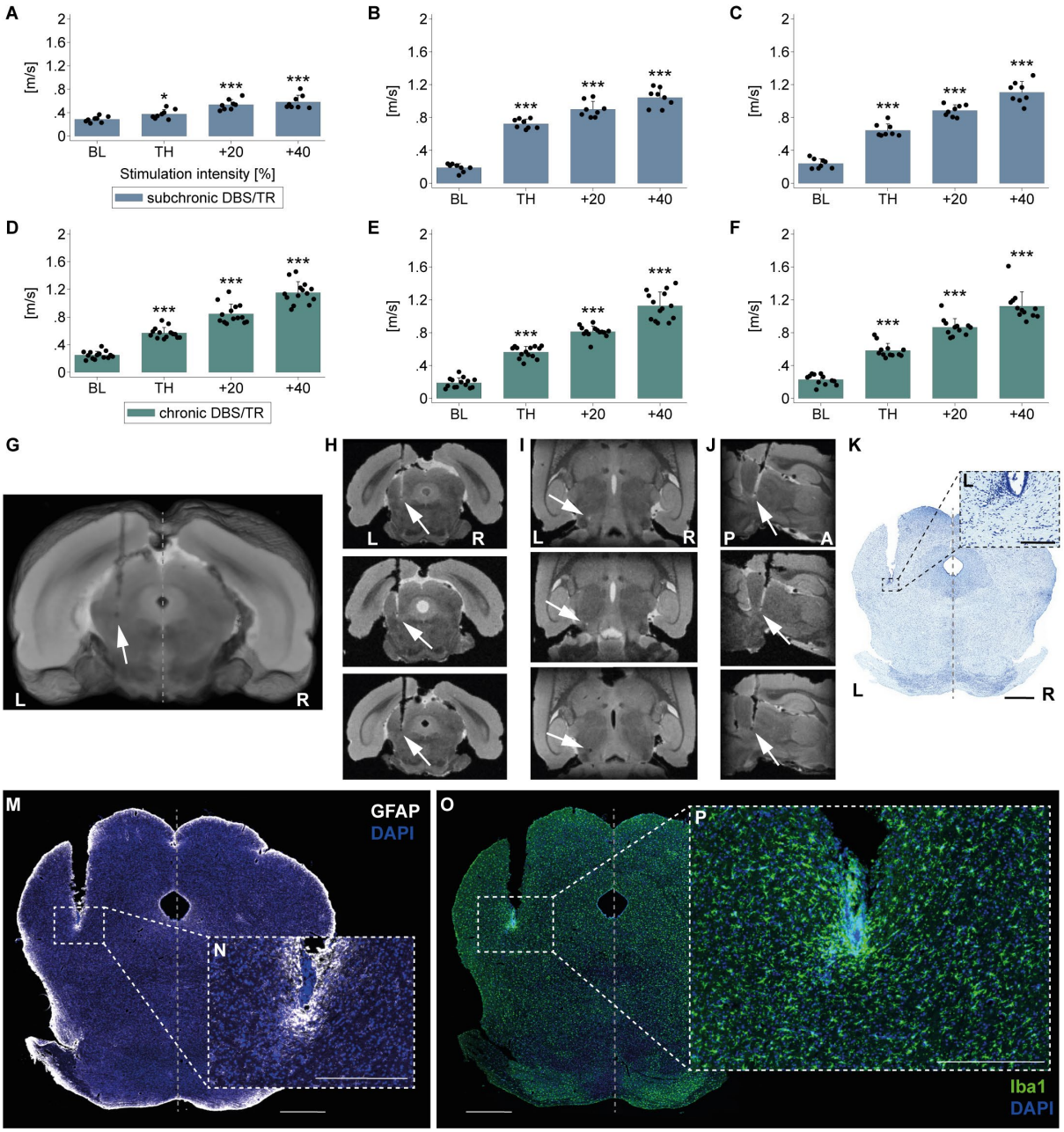

Supplementary Figure 6. Long-term efficacy of CNF-DBS to enhance locomotor speed and minimal perifocal changes upon repeated CNF-DBS. (**A-F**) Long-term functionality of electrodes and preserved efficacy of CNF-DBS to enhance locomotor strength in the open field at all timepoints. (**A-C**) Significant increase in speed during open field locomotion with CNF-DBS (**A**) before and (**B**) after training period, and after (**C**) 4 weeks of retention in subchronic (blue) DBS/TR group (n = 8). (**D-F**) CNF-DBS significantly enhanced locomotor strength in the open field (**D**) before and (**E**) after training period, and after (**F**) retention period of 4 weeks in chronic (green) DBS/TR group (n = 14 in **D**, **E**; n = 12 in **F** due to loss of implants of 2 animals). Asterisks indicate significance of Bonferroni post hoc test comparing speed at each stimulation intensity with baseline performance after one-way repeated measures (intensity)

ANOVA ($P < 0.001$). * ($P < 0.05$), ** ($P < 0.01$), *** ($P < 0.001$). BL = baseline without stimulation. TH = individual motor threshold. Data are represented as mean + SD. Dots represent single animals. X-axis = stimulation intensity expressed as percent of TH. (**G**-**J**) Post-mortem ex-situ 7 Tesla (Bruker BioSpec) magnetic resonance images (3D-FLASH sequence, matrix 100x150x100, 100 µm spatial resolution) of 3 representative DBS/TR animals demonstrate preservation of tissue structure with chronic CNF-DBS. L = left; R = right. A = anterior; P = posterior. White arrows show localization of former electrode tip. (**G**) Coronal volume projection illustrating extent of electrode channel. (**H**) Coronal, (**I**) horizontal, and (**J**) sagittal view of electrode tip. (**K**) Coronal Nissl-stained midbrain section at the center of former electrode channel of a chronic DBS/TR animal illustrating preservation of tissue structure after chronic CNF-DBS. Scale bar: 1 mm. L = left; R = right. (**L**) Magnification shows intact tissue surrounding former electrode tip. Scale bar: 200 µm. (**M**-**P**) Perifocal scarring around the electrode tip was low as shown by immunohistochemistry for glial fibrillary acidic protein (GFAP; primary antibody: rabbit-anti-GFAP, 1:1000, Dako; secondary antibody: donkey-anti-rabbit-Cy5, 1:500, Jackson ImmunoResearch) and ionized calcium-binding adapter molecule 1 (Iba1; primary antibody: rabbit-anti-Iba1, 1:500, Wako; secondary antibody: donkey-anti-rabbit-Cy5, 1:500, Jackson ImmunoResearch), counterstained with DAPI. (**M**) Coronal GFAP-stained midbrain section of chronic DBS/TR animal showing channel of former electrode. Scale bar: 1 mm. (**N**) Magnification of electrode tip demonstrating minimal perifocal gliosis. Scale bar: 500 µm. (**O**) Coronal Iba1-stained midbrain section of chronic DBS/TR animal at the center of former electrode channel. Scale bar: 1 mm. (**P**) Magnification of area surrounding electrode tip demonstrating low perifocal microglia activation. Scale bar: 500 µm. (**G**, **K**, **M**, and **O**) Gray dashed vertical line represents midline. (**G**-**P**) Imaging and histology performed after removal of electrodes; tissue fragments along electrode channel are artifacts generated by removal of electrodes from fixed brains.

References

1. Lein ES, Hawrylycz MJ, Ao N, et al. Genome-wide atlas of gene expression in the adult mouse brain. *Nature*. 2007;445(7124):168-176.
2. Schroeder LE, Furdock R, Quiles CR, et al. Mapping the populations of neurotensin neurons in the male mouse brain. *Neuropeptides*. 2019;76:101930.
3. Ferreira-Pinto MJ, Kanodia H, Falasconi A, Sigrist M, Esposito MS, Arber S. Functional diversity for body actions in the mesencephalic locomotor region. *Cell*. 2021;184(17):4564-4578.e18.
4. Paxinos G, Watson C. *The Rat Brain In Stereotaxic Coordinates: Compact Sixth Edition*. Elsevier, Academic Press; 2009.
5. Watson C, Paxinos G, Kayalioglu G. *The Spinal Cord: A Christopher And Dana Reeve Foundation Text And Atlas*. Elsevier, Academic Press; 2009.
6. Bachmann LC, Matis A, Lindau NT, Felder P, Gullo M, Schwab ME. Deep Brain Stimulation of the Midbrain Locomotor Region Improves Paretic Hindlimb Function After Spinal Cord Injury in Rats. *Sci Transl Med*. 2013;5(208):208ra146-208ra146.